Atmos. Meas. Tech. Discuss.,
doi:10.5194/amt-2017-67-AC1, 2017

Atmospheric Measurement Techniques Discussions

Interactive comment on "Analysis and evaluation of WRF microphysical schemes for deep moist convection over Southeastern South America (SESA) using microwave satellite observations and radiative transfer simulations" *by* Victoria Sol Galligani et al.

Victoria Sol Galligani et al.

victoria.galligani@cima.fcen.uba.ar

Received and published: 1 July 2017

We would like to thank Alan Geer for his insightful comments. Below we address each of the comments made.

Main points

1) In the introduction, or at the end of section 2.2, it would be good to survey all previous

validation of the WRF microphysics and to summarise any known issues.

Section 2.2 has been modified to include more information on previous validations and how these compare with simulations in the present work. A more in-depth review of all previous validation studies is outside the scope of this paper. Please see Section 2.2 in the new paper version. I copy below the new paragraph:

"Validation techniques of these schemes depend upon the availability of observations. In-situ measurements are essential for detailed and direct microphysics validations, such as particle size distributions and liquid/ice water content. However, these observations are limited to certain field campaigns as well as certain parts of the storms. On the other hand, satellite observations can cover this gap if they are widely available and are very useful for model validation. Figure 4 shows that the WSM6 and the WDM6 schemes model similar hydrometeor mass loadings and storm morphology. This is expected as the WDM6 is developed from the processes in the WSM6 scheme. The THOM scheme, on the other hand, shows much higher snow contents as reported in many studies (e.g., Kim et al., 2013 and Gallus and Pfeifer, 2008). Figure 5 further shows the domain-averaged vertical distribution of the hydrometeor contents modelled by the different schemes between 18:00 and 19:00 UTC. Units are in g/kg for all the species. Both Figure 4 and Figure 4 show a comparable behaviour in the frozen phase (ice, snow and graupel) in the WSM6 and WDM6 schemes. This is expected because the WDM6 scheme follows the cold-rain processes of the WSM6 scheme and the added processes in the WDM6 do not affect the frozen phases directly (Lim et al, 2010). Comparing the warm-rain processes of the WSM6 and WDM6 schemes, Figure 5 shows an increase of the WDM6 rainwater mixing ratio below 5 km with less cloud droplet mixing ratios, as reported by Kim et al., 2013 who studied a typhoon event and reported that the liquid phase in the WDM6 scheme produced a significantly larger amount of rainwater but smaller cloud droplet mixing ratio. Various studies have shown that the double-moment approach in the WDM6 scheme may help to achieve a more realistic simulation of convective rain and rainfall retrievals, as the rain number concen-

tration plays an important role in determining the precipitation rate and storm morphology because it modulates the related microphysics terms, in particular, the evaporation rate (Morrison et al., 2009, Li et al., 2009a,b, Lim and Hong, 2010). Figure 4 shows that the the THOM scheme predicts the smallest amount of rain water, while Figure 5 further shows that the THOM scheme is dominated by snow throughout the vertical profile. These conclusions are also reached by Kim et al., 2013. The THOM scheme has a maximum cloud water content between 8 and 10 km. This peak of enhanced cloud water content is found within and around strong convective updrafts (Otkin et al., 2003). In order to compare the distribution of the frozen hydrometeor species among the total frozen phase for each scheme, Figure 5 additionally shows the mean vertical profile of the total frozen content (i.e., ice+snow+graupel, shown in light blue). The total frozen content is comparable in magnitude in all the schemes analyzed but since each scheme has different intrinsic assumed characteristics and microphysical processes, they partition the total content in different ways between graupel, cloud ice, and snow. The THOM scheme has the most prominent vertical structure. Note that very similar remarks can be drawn from the model simulations at 07:00 UTC in coincidence with the available TMI observations (not shown)."

2) A minor but repeated issue (e.g. lines 142-144; lines 468, 478, 495) is the attribution of brightness temperature (TB) depressions at low frequencies (e.g. 85 GHz or less) uniquely to scattering. Over land, at low frequencies, cloud water and particularly rain (and possibly snow too) can generate TB depressions through absorption and emission pushing the weighting function up to colder layers in the atmosphere. It would be good to examine more closely whether it really is scattering causing the TB depressions in all cases. Incorrect modelling of the cloud water or rain could also contribute to mismatches between observations and simulations.

Thank you for raising this point up for discussion. I agree that at low frequencies, cloud water and rainwater can generate TB depressions through absorption and emission by pushing the weighting functions up to colder layers in the atmosphere. In fact, there is

a contribution of these processes in the cases examined, especially at the lowest frequencies (especially below 37 GHz). This was examined more closely, but not shown. The transects simulated in Figure 7 for TMI were simulated with no population of frozen species. For example, for WSM6(DDA=sector) simulations at the 19 GHz channel, TBs simulated without the frozen phase did not change significantly (5K warmer TBs). This means that at 19 GHz the most important contribution to the TB depressions simulated is liquid water absorption, emissions and scattering. These liquid phase only TBs simulated with the WSM6 scheme are 10K colder than those observed by TMI. This bias is larger for the WDM6 scheme which has a larger simulated rain water path. This is the order of magnitude that incorrect modelling of rain water can contribute to biases in simulated TBs at 19 GHz. The same test was run for the THOM scheme. For the THOM scheme, TBs simulated without the frozen phase changed even less significantly (approx. 3K warmer TBs for DDA=sector habits) and remained closed to the observed TBs. At 37 GHz, a 10K difference is observed between simulations with and without the frozen phase for WSM6(DDA=sector), and both simulations are comparable to the observed TBs as the observed TBs lie between the simulations with and without the frozen phase for the WSM6(DDA=sector). For the THOM scheme, TBs simulations without the frozen phase were 12K warmer than those with the frozen phase. Considering that the THOM scheme simulations with all the phases are shown to be close to the observed TMI observations, those simulations without the frozen phase were shown to be warmer than those observed. At 85 GHz, however, the contribution of frozen scattering is much stronger and a 60K difference is found between simulations with and without the frozen phase for WSM6(DDA=sector). TB simulations without the frozen phase are 60 K warmer than those observed by TMI. This shows that frozen phase scattering is key to explain the observed TBs. The DDA sector habit has been shown to be the least scattering habits when used through the equal mass approach with the WSM6 scheme. If the above exercise is repeated with DDA=6-b rosettes for example, differences between the simulations with and without the frozen phase are much larger. At 85 GHz, it is evident that scattering causes the TB depressions. A similar behaviour

is observed for the THOM scheme simulations. The higher the microwave frequency of the (window) channel, the higher the sensitivity to scattering of the frozen phase, but even a the 37 GHz channel, the 10K difference is an important contribution from frozen scattering. As discussed above, it can be debated that the WSM6/WDM6 schemes show incorrect modelling of the liquid water phase from the 19GHz simulations. However, the uncertainties associated with incorrect modelling of the cloud water and rain are much smaller than those associated with incorrect modelling of the frozen phase as evidenced by the large sensitivity to snow shape for example. In addition, this are extremely severe convection cases with a large IWP. At 19 GHz, differences are due to the incorrect modelling of the liquid water phase in the WSM6/WDM6.

To be more thorough in the text the following modifications have been made:

Lines 142-144: The text reads “The highly scattering MCS event is evidenced by brightness temperature depressions at the higher frequency channels ($\geq$37 GHz). At the lower frequency channels ($\leq$37 GHz), TMI is mostly sensitive to surface emission, and cloud absorption and emission.”

Lines 468, 478: These lines, deals with the differences in the WSM6/WDM6 simulations with different DDA habits. These differences in TB arise from the scattering signal of graupel+snow, which are strong enough to be seen at 19 GHz. Simulations without the frozen phase show that simulations are up to 10K colder for the sector snowflakes. This means that a bias also exists due to the liquid phase WRF model outputs. This is not observed in the THOM scheme, where simulations at 19 GHz with and without the frozen phase are very close to those observed by TMI. The text has been slightly modified: “At 19 GHz, all DDA habits produce excessive scattering for the WSM6 and WDM6 simulations, where the dendrite and sector habits simulate the warmest TBs closest to the observed reference TBs, and the thick hexagonal plates and the block, long and short hexagonal columns (not shown) are the most scattering habits, producing the coldest TBs, followed by the thin hexagonal plate and the rosettes (only the 6-b rosette is shown). On the other hand, all DDA habits in the THOM scheme simulations produce

similar TB depressions to those observed. The large depression observed at 19 GHz in the WSM6/WDM6 simulations is due to the high IWP graupel frozen phase contents simulated by WRF. Simulations for the WSM6 show larger brightness depressions at 19 GHz as they have a larger IWP graupel content. Note that simulations without the frozen phase show simulated brightness temperatures closer to those observed, but still show a significant cold bias (10 K). Note that due to the small brightness temperature depressions simulated using the THOM scheme, the signal coming from the lake at approximately -32.9$ˆo$ can be observed at 19 GHz, while simulations using the WSM6/WDM6 schemes are dominated by excessive scattering and consequently frozen phase scattering cloud signals dominate all surface signals. Note that although the THOM scheme is predicting the largest amount of integrated snow content, it does not necessarily produce the largest brightness temperature depressions.”

3) A feature of the equal-mass approach is that it changes the relative amount of scattering generated by the Liu particles, in one case making the sector snowflake the most scattering particle (e.g. lines 506-510; 537-541). This is one of the most interesting aspects of the study and it could do with further exploration in the text (and possibly more figures) to explain exactly how this occurs (note the lack of labelling on Fig. 6 has not helped here - minor point 8).

Thank you for bringing up this central issue for discussion. Figure 6 has been modified and a futher figure has been added (Both attached in this response). Please below the legends for these figures:

Figure 6: "Left: The corresponding equal mass DDA habit size calculated from Equation 3 for WRF (top) WSM6 and WDM6 and (bottom) THOM schemes. Right: The normalized scattering cross sections of the equal mass DDA sized habits D’max as a function of Dmax at 150 GHz and at 263 K for the WSM6/WDM6 (solid lines) and the THOM scheme (dashed lines)."

Figure 7: "Left: The vertical profiles for the WSM6 and THOM snow mixing ratios

(g/m3) for the corresponding pixel of maximum snow water path in an MHS transect explored in Section 4 and introduced in Figure 4(i) above. Right: The resultant vertical profile of the bulk scattering properties at 150 GHz for the WSM6 (solid lines) and THOM (dashed lines) schemes, i.e., the extinction coefficient at each vertical level. The bulk optical properties have been computed at each vertical level by integrating the scattering properties of the equal mass Liu (2008) particle habits over the size distributions of interest."

The new now text reads:

"In Equation 3, D is inferred from WRF parameterizations and is used in the particle size distribution. D'max is the corresponding equal mass DDA habit size used to describe the scattering properties of the WRF species consistently. This discussion is important since particle size is a key parameter in single scattering calculations. Figure 6(a) and (b) shows the corresponding equal mass D'max for a selected number of Liu (2008) habits when using the WSM6/WDM6 and THOM schemes respectively. The choice of DDA habits shown is a result of regrouping certain habits that behave similarly, such as the thin hexagonal column, the long hexagonal column, the short hexagonal column and the thick hexagonal column, or the bullet rosettes. Note that the included black dashed line represents unity. As shown in Figures 6(a) and 6(b), for a given maximum particle dimension in WRF, the equal mass DDA habit D'max can be very different for each of the Liu (2008) habits. Figures 6(a) and 6(b) also show that the equal mass DDA habit D'max is larger when using the WSM6 and WDM6 schemes than when using the THOM scheme. This is expected due to the intrinsic ÏśS differences in these schemes. For the most compact habits of the DDA database, like columns and plates, the difference in D'max between the WSM6/WDM6 and the THOM schemes is the smallest, while the largest differences are seen for the dendrite and sector habits, especially at larger Dmax. The thin hexagonal plates for example, have equal mass D'max diameters above Dmax for the WSM6/WDM6, and equal mass D'max diameters below Dmax in the THOM scheme. The 6-b rosette equal mass

D'max is larger for the WSM6/WDM6 schemes but close to unity for the THOM scheme. Figure 6(c) shows as a function of Dmax the normalized scattering cross sections at 150 GHz of the corresponding equal mass WSM6/WDM6 (THOM) D'max habits in solid lines (dashed lines). Figure 6(c) shows that in general, WSM6/WDM6 normalized scattering cross sections are larger than the THOM scheme, specially at the larger Dmax values where the equal mass size approach starts to yields larger D'max values for the WSM6/WDM6 than the THOM scheme (i.e., greater scattering). Special attention needs to be made for the sector snowflakes, because as shown in Figure 6(c) the WSM6/WDM6 and THOM normalized scattering cross sections are similar at large diameters. This is due to the maximum dimension of sector habits in the DDA database: 1 cm. The WSM6/WDM6 D'max values are capped at this value. Figure 6(c) further shows that the thin hex. plt. and 6-b rosettes dominate at larger diameters, while at smaller diameters the sector habits are the most scattering. An analysis of the dependence of the scattering cross sections with frequency is shown to increase with frequency as expected (not shown). To further study the scattering properties with this approach to consistently simulate realistically the radiative properties of hydrometeors with WRF parameterizations, Figure 7 shows the bulk scattering properties for a specific point of the transect introduced in Figure 4(i) above. This is a transect of MHS observations that is discussed in Section 4 below. Figure 7(a) shows the vertical profiles for the WSM6 and THOM snow mixing ratios (g/m3) for the corresponding pixel of maximum snow water path in the transect. Figure 7(b) shows the resultant vertical profile of the bulk scattering properties (e.g., the extinction coefficient βe) at 150 GHz for the WSM6 (solid lines) and THOM (dashed lines) Field et al., 2005 snow particle size distributions, i.e., the extinction coefficient at each vertical level. This βe parameter is calculated by integrating the extinction cross section σe(D) across the particle size distribution N(D) at each vertical level:

βe=$\int \sigma$e(D)N(D)dD

The integrated bulk properties showed in Figure 7(b) include the effects of using the

equal mass habit approach discussed above and the particle size distribution. Note that the WDM6 scheme is not shown as it has the same snow parameterizations as the WSM6. As expected, extinction (and scattering) increases with frequency (not shown) and snow water content. Not shown is the asymmetry parameter which gives an overall description of the phase function, i.e., the angular redistribution of scattered radiation. In contrast to the Liu (2008) habits, the low density Mie sphere model (not shown) gives very strong forward scattering for high snow water contents. The Liu (2008) habits produce more balanced forward and backward scattering. Although not shown graphically, analysing the sensitivity of these bulk scattering properties with frequency indicates that these conclusions are broadly true for the microwave range of interest in the present study. As the scattering increases, so do the differences between the bulk WSM6/WDM6 and THOM properties. Both the particle size distributions and how D'max differs from Dmax play an important role. Figure 7(b) illustrates the complex nature of evaluating the relative importance of these two effects. In the WSM6 scheme, the thin hexagonal plates and the 6-b rosette are the most scattering habits, while the sector and the dendrite habits are the least scattering habits. For the THOM scheme, on the contrary, the sector habit is the most scattering. This is explained by the differences in the particle size distributions. The Field et al., 2005 snow particle size distribution has a larger number of smaller hydrometers and a smaller number of larger hydrometers than the WSM6/WDM6 snow particle size distribution. According to the analysis of Figure 7(c), the scattering cross sections behave differently for smaller and larger diameters. At larger diameters, the thin hexagonal plate is the most scattering habit, while at smaller diameters, the sector habit is the most scattering habit."

4) Some of figures 16-20 could be considered for reduction, as they mainly repeat and confirm the results of the case study in section 4. I think that they are useful for reference of how the different cases behave in terms of the radiative transfer simulations.

5) Some figures are too small and fuzzy - e.g. Figure 3 longitude and latitude legends; Figs 9, 10, 11, 12. Some figures have been made larger. The fuzzy effect I believe is

due to the quality of figures downgraded at some point.

Minor points

1) Line 232: "As expected WSM6 and WDM6 schemes model similar ...loadings": for the benefit of the reader, could the reason be restated here, instead of just saying "as expected"?

This paragraph has been modified based on RC1 Point (1) and the text now reads: "Both Figure 4 and Figure 5 show a comparable behaviour in the frozen phase (ice, snow and graupel) in the WSM6 and WDM6 schemes. This is expected because the WDM6 scheme follows the cold-rain processes of the WSM6 scheme and the added processes in the WDM6 do not affect the frozen phases directly (Lim and Hong, 2010)"

2) Line 308-311: "The only computationally realistic approach is to assume a one shape model". This statement could be challenged: an ensemble of particles could be used without much additional computational effort - for example something like the Baran (2009) ensemble. http://ac.els-cdn.com/S0022407309000661/1-s2.0-S0022407309000661-main.pdf?_tid=2084b234-506d-11e7-b2db-00000aacb360&acdnat=1497381708_72b9189f7ca88301717bad59c21a3295

The model in Baran (2009) consists of six ice crystal shapes for cirrus clouds: a simple hexagonal ice column and a six-branched bullet-rosette (the smallest ice crystals in the PSD). As the ice crystal maximum dimension increases so does the ice crystal complexity by forming aggregates of hexagonal ice columns, which are arbitrarily attached to other hexagonal elements, forming three, five and eight element aggregates until finally, a chain of 10 hexagonal elements is constructed. This 10 element hexagonal ice aggregate represents the largest ice crystals in the PSD. The PSD is sub-divided into six equal sections with each ice crystal shape distributed within each section, so the simple hexagonal ice column and 10 element ice aggregate is distributed within the first and sixth sections of the PSD. It is true that something like this could be implemented in the context of larger hydrometeors, not pristine ice crystals like in cirrus clouds, without

additional computational effort. This is however, outside the scope of the paper. The present work exploited the existent Liu (2004) DDA scattering databases, and choosing different shapes for different size ranges would be arbitrary and lack physical support. We strongly agree that an ensemble could be developed and tested without additional computational effort.

3) Lines 338-339, 445-447. In both these areas the question arises "are both snow and graupel simulated using the same Liu particle habit?"The answer is probably yes, but it would be worth (re?)-stating this for the benefit of the reader.

Yes. This has been re-stated again.

4) Line 524: "The higher the window channel" - higher what? Frequency?

Thank you! This has been corrected to “The higher the frequency of the window channel”

5) Line 602-603: "WDM6 leads to excessive scattering at > 19 GHz". This is not obvious to me. At 37 GHz WDM6 is the only model to generate TB depressions as low as observed, albeit over a wider area than observed. At 89 GHz, none of the schemes generates sufficient TB depression.

This is true. It has been removed.

6) Line 603-604: "Figure 14 shows good agreement" - this could be restated in more depth and a little more critically. For example there is the broader spread of TB depressions generated by THOM, versus perhaps too-narrow areas of TB depression from the other schemes. As in Fig. 13, none of the schemes have deep enough depressions at 89 GHz.

The following has replaced those lines: “Despite errors in the location and coverage of the spatial structures of the cloudy fields modelled by WRF, the results depicted show that the three WRF microphysics schemes can be used to simulate the observed brightness temperature depressions provided special care is taken to represent the

scattering properties of the snow and graupel species. At 19 GHz, the THOM scheme does not have deep enough brightness temperature depressions as observed, while at 37 GHz, the WDM6 scheme is the only model to generate brightness temperature depressions as low as observed, albeit over a wider area than observed. At 89 GHz, none of the schemes reach deep enough brightness temperature depressions as observed. MHS simulations have a higher sensitivity to frozen scattering. Figure 15 shows good agreement between the three microphysics schemes and MHS observations. The THOM scheme, however, has a broader spread of TB depressions, versus the too-narrow areas of TB depression from the other schemes. Similarly to Figure 14, Figure 15 also shows that at 89 GHz none of the schemes reach deep enough brightness temperature depressions as observed.”

7) Line 709-710: poor wording in this sentence suggests that the Liu habits all have the same bulk scattering properties - please rephrase.

The sentence “The bulk scattering properties of the Liu (2008) habits are similar for the WSM6 and WDM6 schemes, but different to the THOM scheme” has been rewritten as “The resultant bulk scattering properties of each of the Liu (2008) habits under the WSM6 scheme is similar under the WDM6 scheme, but different under the THOM scheme.”

8) Figure 6 has no key for the black dashed line in the left panels, or the significance of solid versus dashed in the right panel.

Thank you. This has also been raised by the other reviewer. Thi Figure has been modified in reference to RC1 point (3).

9) Figure 8 needs a key to the black dashed line.

Thank you. This has been added. It is also referenced in the legend.

10) The many figures featuring chi-squared tests are not all consistent in terms of the y axis labelling: some use "#()" (not explained) and some "E()" (explained in the text)

Thank you for pointing this out. This has been corrected to use Ei as used in the text. The "#()" only belonged to the histograms.

Grammar points

1) There is a repeated error in the text that writes "South Easter" instead of the correct "South Eastern"

Thank you for pointing this out. It has been corrected.

2) Line 165: "described" should be "describe"

Thank you for pointing this out. It has been corrected.

3) In a few places, "sensibility" is used in place of the correct english term "sensitivity".

Thank you for pointing this out. It has been corrected.

4) Line 230 "similarly to TMI observations" is hard to understand and the sentence should be rewritten for clarity.

This sentence has been rewritten as: “A close examination of MHS (and TMI) observations in Figure 2 (Figure 1) and the WRF cloud outputs in Figure 4 (not shown for TMI passage time), however, reveals that the cloud system modelled by WRF is slightly time lagged and misplaced with respect to the observations.”

Interactive comment on Atmos. Meas. Tech. Discuss., doi:10.5194/amt-2017-67, 2017.

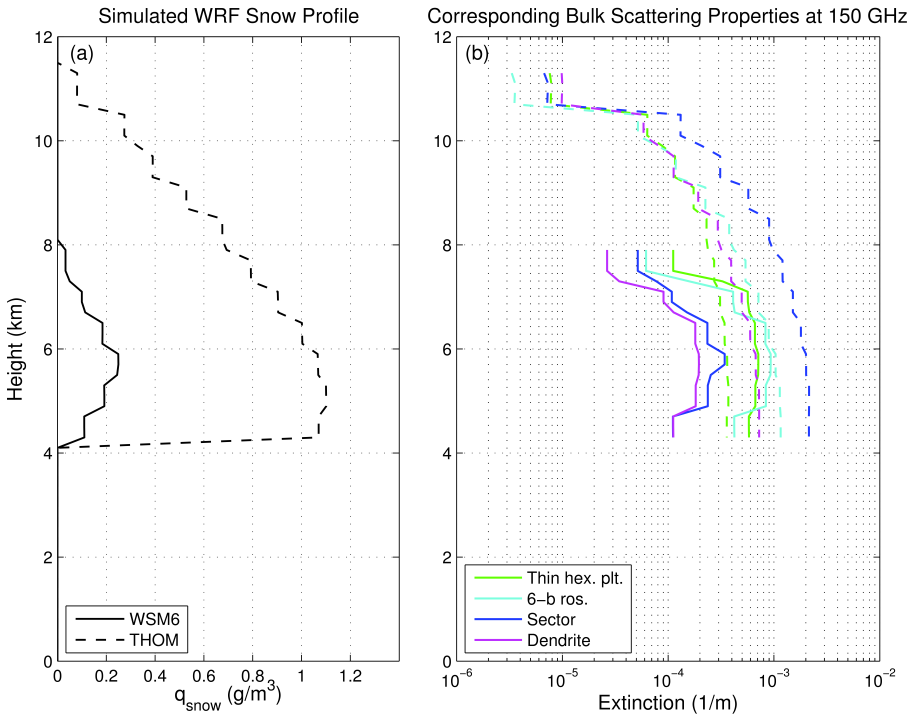

Fig. 1. Figure 7

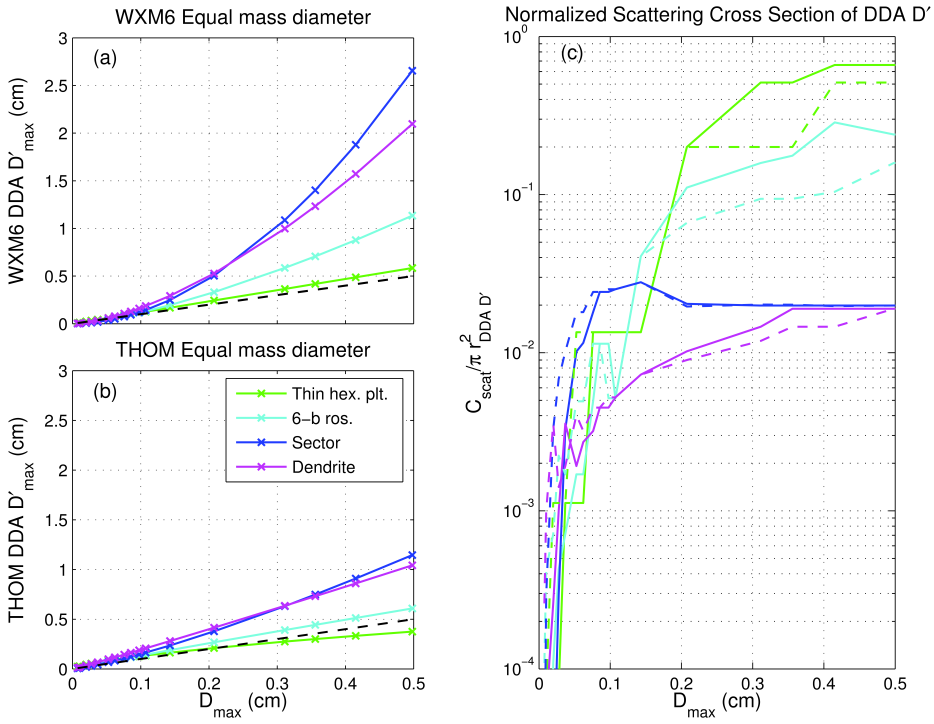

Fig. 2. Figure 6